PREPARATION, CHARACTERIZATION, THERMAL BEHAVIOUR AND DC CONDUCTIVITY OF NANO-POLYANILINE AND POLYANILINE-MULTI WALLED CARBON NANOTUBE NANOCOMPOSITES

[1]Kingsley Kema Ajekwene[*], [2]Jelmy E Johny and [3]Thomas Kurian
[1]Research Scholar, [2]Post Doc Fellow and [3]Professor
[1, 2,3]Department of Polymer Science and Rubber Technology, Cochin University of Technology, Kochi – 682 022, Kerala State, India.
[1]Department of Polymer and Textile Technology, Yaba College of Technology, P.M.B. 2011, Yaba, Lagos, Nigeria.

Abstract: ***Conducting polyaniline (PANI) in nano dimension was prepared in presence of aqueous hydrochloric acid (HCl) or toluene sulfonic acid (TSA) as doping agents and ammonium persulfate (APS) as oxidizing agent. Composites of the PANI and multi walled carbon nanotubes (MWCNT) were prepared by in situ polymerization technique at room temperature. The structural composition, morphology, thermal decomposition behavior and conductivity of PANI and the composites were investigated. Studies include Fourier transform infrared (FTIR) spectroscopy, scanning electron microscopy (SEM), transmission electron microscopy (TEM), x-ray diffraction (XRD) pattern, uv-visible spectroscopy and thermogravimetric analysis (TGA). The electrical conductivity of the PANI-MWCNT composites as well as the pure PANI was measured by conventional four-probe method. The electrical conductivities of the two PANIs show that nano PANI-TSA has a higher conductivity (0.824 S/cm^{-1}) compared to PANI-HCl (0.478 S/cm^{-1}). PANI-MWCNT composites displayed much higher electrical conductivity (4.17 S/cm-1) compared to neat PANI.***

Keywords: ***Nano polyaniline, carbon nanotubes, chemical oxidative polymerization in situ polymerization, thermal stability, electrical conductivity.***

1.0 INTRODUCTION

Polymers were regarded as electrically non-conducting materials until Shirakawa et al. in 1977 [1] discovered significant electrical conductivity in polyacetylene (PA) after its oxidation in presence of iodine vapour. Conducting polymers are organic polymers that conduct electricity as they possess electrical properties like that of metals (metallic conductivity) and semiconductors. They display several other characteristics of organic polymers such as lightweight, lower cost, resistance to corrosion and chemical attack, flexibility and greater workability [2-6]. They are widely used in many electrical/electronic devices and for a myriad of applications. Among different conducting polymers, polyaniline (PANI) is the most versatile owing to its low cost, low specific mass, thermal/chemical stability and high conductivity [7, 8]. These properties can be enhanced to meet the requirements of present day sophisticated technologies in order to further expand their application likelihoods. Composite preparation is one of the ways to improve the conductivity of conducting polymers. Polyaniline/carbon nanotubes (PANI/CNTs) based composites have been widely explored in which the charge-transfer activities between the two components lead to considerable improvement in conductivity [9]. PANI/CNTs nanocomposites are prepared either through grafting PANI macromolecules on the CNTs or through in situ polymerization of aniline monomer in CNT dispersion. They possess impressive and interesting structural, mechanical, electrical and electronic, optical, thermal and chemical characteristics due to their small size and mass [10, 11].

In this work we report the synthesis of PANI in nano dimensions through chemical oxidative polymerization of aniline using HCl or TSA as dopants and APS as oxidant. Nanocomposites of polyaniline and MWCNTs were prepared by in situ polymerization. Functionalized nanotubes are easier to disperse in organic solvent and water, which can improve the dispersion of the MWNTs within polymer matrix [12-15]. For this purpose, we have used pristine CNT, amine functionalized multi-walled carbon nanotubes (ACNT) and carboxylic acid functionalized multi-walled carbon nanotubes (CCNT) as fillers in the composites.

2.0 MATERIALS AND METHODS

2.1 Materials

Chemicals and solvents: Ammonium persulphate (APS), p-toluene sulfonic acid monohydrate (TSA) and aniline obtained from Sigma Aldrich Chemical Company were of very high purity (99.9%). Hydrochloric acid (HCl) 98%, and acetone were obtained from Spectrochem Pvt Ltd, Mumbai, India. The aniline was distilled before use. All other materials were used without any pre-processing.

Carbon nanotubes (CNT): pristine CNT, carboxylic acid functionalized MWCNT (CCNT) and amine functionalized MWCNT (ACNT) were obtained from AdNano Technologies Pvt. Ltd., Bangalore, Karnataka, India.

2.2 Methods

2.2.1 Synthesis of polyaniline (PANI)

Nano polyaniline was prepared by chemical oxidative polymerization of 200 **µl** aniline using 0.66g of ammonium per sulfate dissolved in 1.8 ml water as initiator in the presence of 40 mL aqueous solution of 1M HCl at room temperature for 12 hrs. The polymer formed was

washed with distilled water, dilute HCl solution and finally with acetone until the filtrate becomes colourless to remove excess HCl, oxidant, aniline and oligomers. The green coloured precipitate was then dried in vacuum oven at 50 ^{O}C for 24 hours. The dried mass was ground to fine powder using mortar and pestle. The prepared polyaniline is designated as nano PANI-HCl. In order to determine the influence of the novel formulation on the dimensions of the synthesized nano PANI-HCl, polyaniline was also prepared in bulk dimension by polymerizing 20 ml aniline using 66g of ammonium per sulfate dissolved in 180 ml water as initiator in the presence of 400 ml aqueous solution of 1M HCl with stirring at room temperature for 12 hrs and designated as bulk PANI-HCl. To confirm the dimensions, the morphology of both the nano and bulk PANI-HCl were analyzed using SEM and TEM.

The same reaction of nano PANI-HCl was repeated with 1 M TSA as dopant keeping all other reactants the same and designated as nano PANI-TSA.

2.2.2 Preparation of PANI-MWCNT composite

Hybrid composites of PANI-MWCNTs was prepared by in-situ chemical oxidative polymerization of 0.2g aniline using 0.66g of ammonium per sulfate dissolved in 1.8 ml water as initiator in the presence of 40 ml aqueous solution of 1M TSA as dopant in the presence of MWCNT in three forms viz pristine CNT, carboxylic acid functionalized (CCNT) and amine functionalized (ACNT). The concentration of MWCNTs was varied as 0.05g (25%), 0.1g (50%), 0.15g (75%), 0.2g (100%), 0.25g (125%), and 0.3g (150%) in the reaction mixture of aniline-TSA. Therefore, the ratio of aniline-MWCNTs is 1:0.25, 1:0.5, 1:0.75, 1:1, 1:1.25, and 1:1.5. The MWCNTs were first refluxed in aniline monomer-dopant acid solution by ultrasonication to disperse them well, and then PANI/MWNTs composite was synthesized by in situ polymerization.

2.3 Characterizations

The morphology and microstructure of the samples was examined by JEOL Model JSM - 6390LV SEM and JEOL/JEM 2100 TEM. The Fourier transform infrared (FTIR) spectra of samples were recorded from KBr sample pellets using a Thermo Nicolet Avatar 370 FTIR spectrometer. The compositional state of the samples was determined using X-Ray Powder Diffractometry (XRD) Bruker AXS D8. The optical absorption by the sample in the UV and visible region was measured with Varian Cary 5000 UV-Visible spectrophotometer in the spectral range 225-1000 nm. Thermogravimetric analysis (TGA) was performed on a Perkin Elmer STA 6000 thermogravimetric analyzer to determine decomposition and transition temperatures, and thermal stabilities of the samples. The electrical properties of the PANI samples were measured by four probe technique (D.C conductivity) using sensitive digital electrometer type Keithley Agilent 616.

3.0 RESULTS AND DISCUSSIONS

3.1 Scanning Electron Microscopy (SEM)

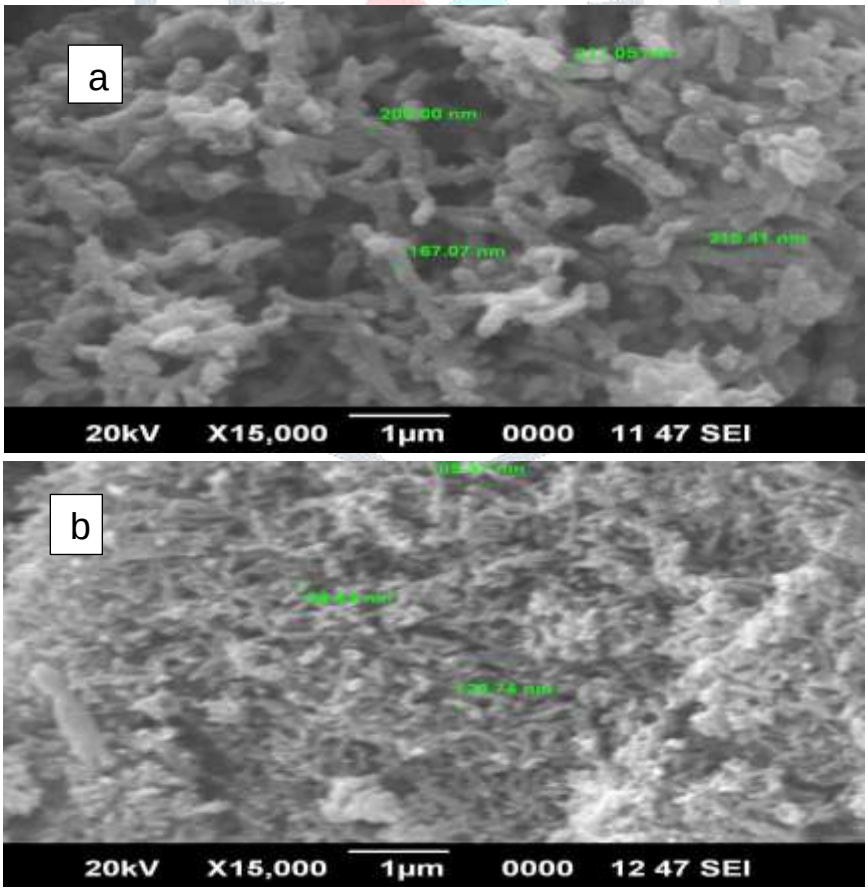

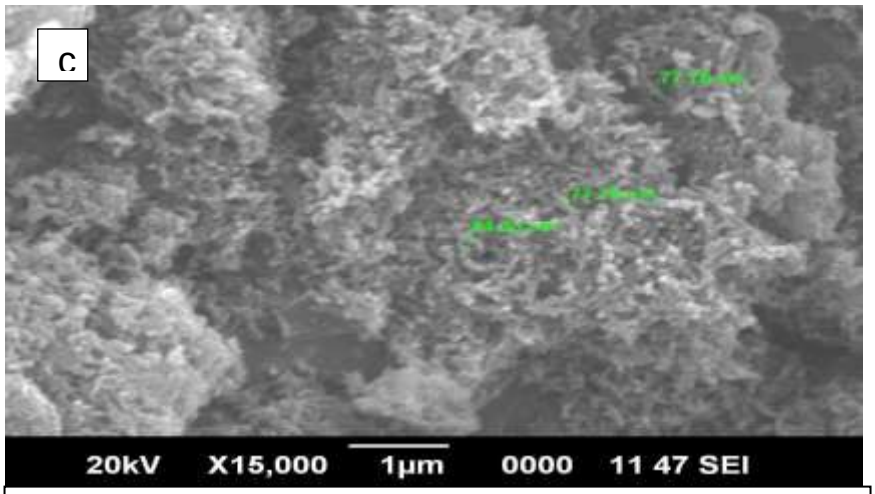

Fig 1. SEM micrographs of PANI: (a) Bulk PANI-HCl (b) Nano PANI-HCl (c) Nano PANI-TSA.

Figures 1a, 1b and 1c show the SEM micrographs of bulk PANI-HCl, nano PANI-HCl and nano PANI-TSA respectively. All the micrographs reveal the irregular granular morphology of the synthesized polyaniline. Bulk PANI-HCl has a porous structure with particle size of 217 nm. The micrographs of nano PANI-HCl and nano PANI-TSA reveal that the synthesized polyaniline comes under nanodimension with an average particle size of 85 nm and 77 nm respectively.

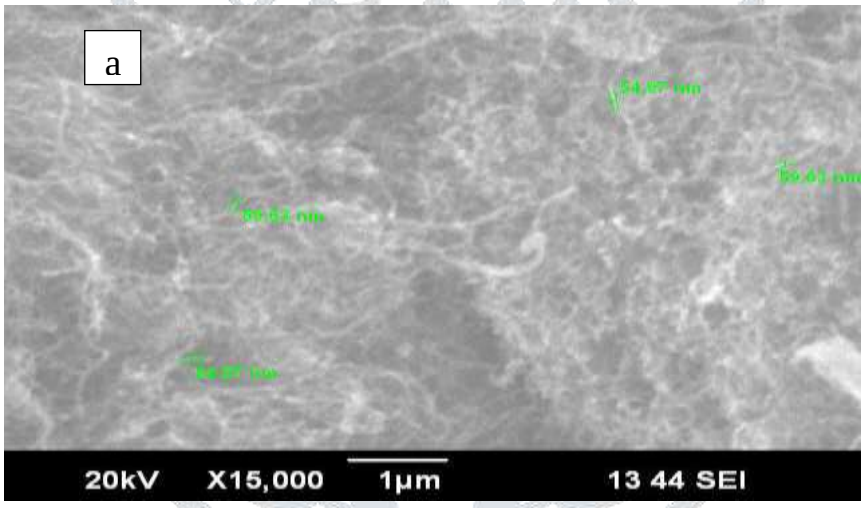

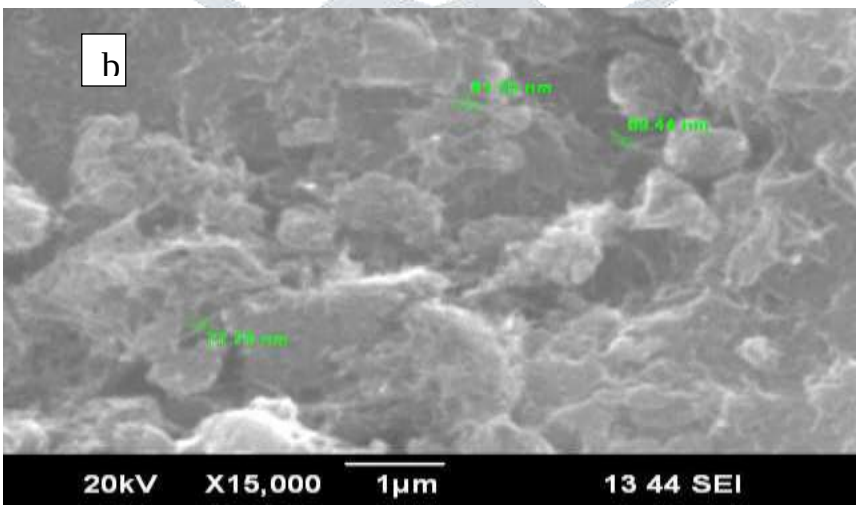

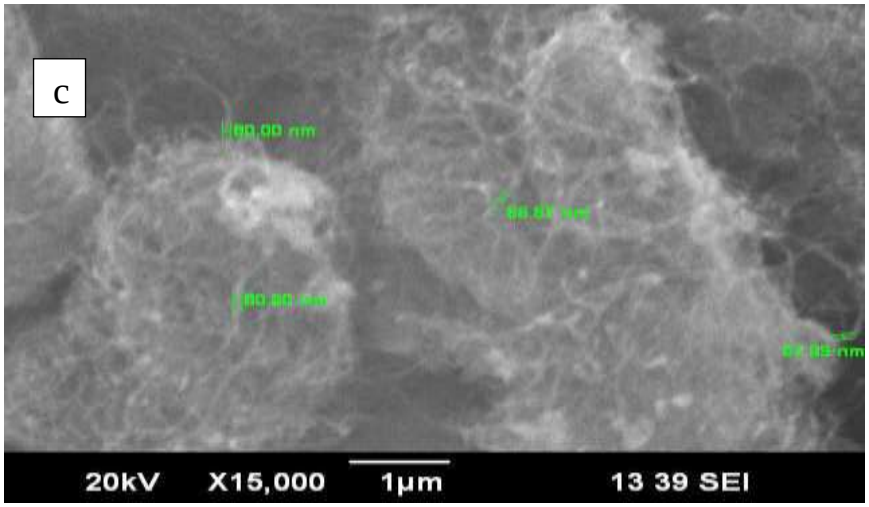

Fig 2. SEM micrographs of MWCNT: (a) Pristine CNT (b) ACNT (c) CCNT.

The SEM micrographs of pristine CNT, ACNT and CCNT samples are presented in Figures 2a, 2b and 2c. Fibrous structures are observed to be homogenous within the whole volume of the MWCNTs studied. The outer diameter of pristine CNT, ACNT and CCNT is found to be 54 nm, 77 nm and 66 nm respectively. The functionalized MWCNTs (ACNT and CCNT) have greater diameter due to the presence of bulky functional groups grafted on its surface. The agglomeration observed in ACNT may be due to the presence of the phenyl amino groups on the surface of ACNT which enhances its tendency to form strong intermolecular hydrogen bonds between CNTs [16, 17].

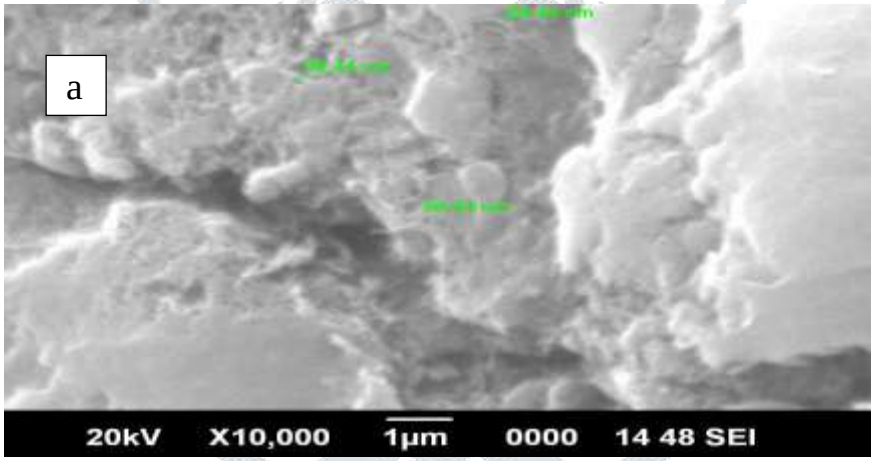

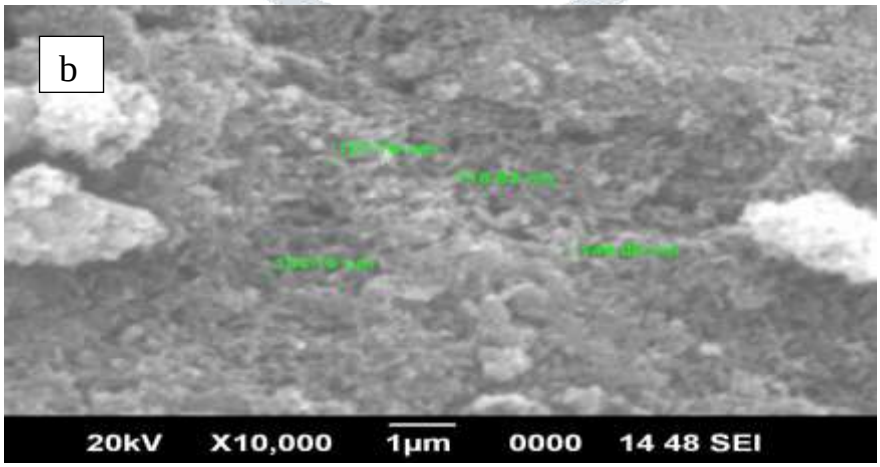

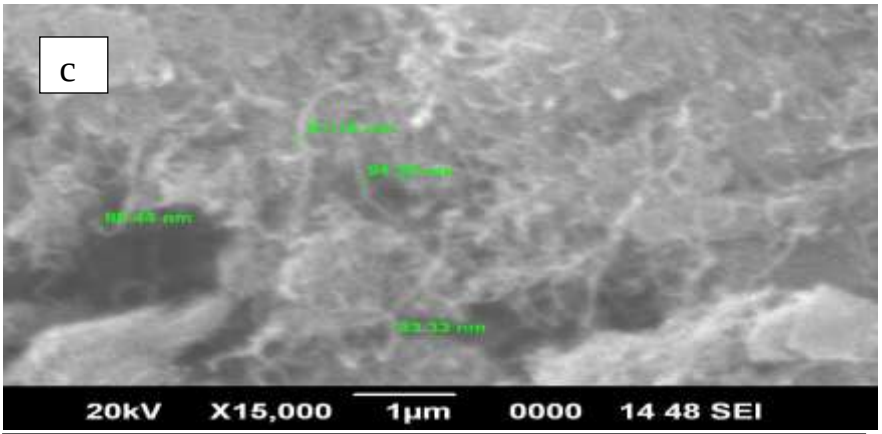

Fig 3. SEM micrographs of PANI-MWCNT: (a) PANI-Pristine CNT (b) PANI-ACNT (c) PANI-CCNT.

The SEM micrographs of PANI-(pristine CNT, ACNT and CCNT) samples are presented in Figures 3a, 3b and 3c. It is clear from the figures that the coiled rod like structures of MWNTs are well dispersed in the PANI matrix. PANI macromolecules are uniformly distributed on the surface of MWNTs forming a tubular shell of the composites [18]. However, Figure 3a (PANI- pristine CNT) shows agglomerations of PANI which may be due to its weak interaction with polyaniline compared to ACNT and CCNT.

3.2 Transmission Electron Microscopy (TEM) Analysis

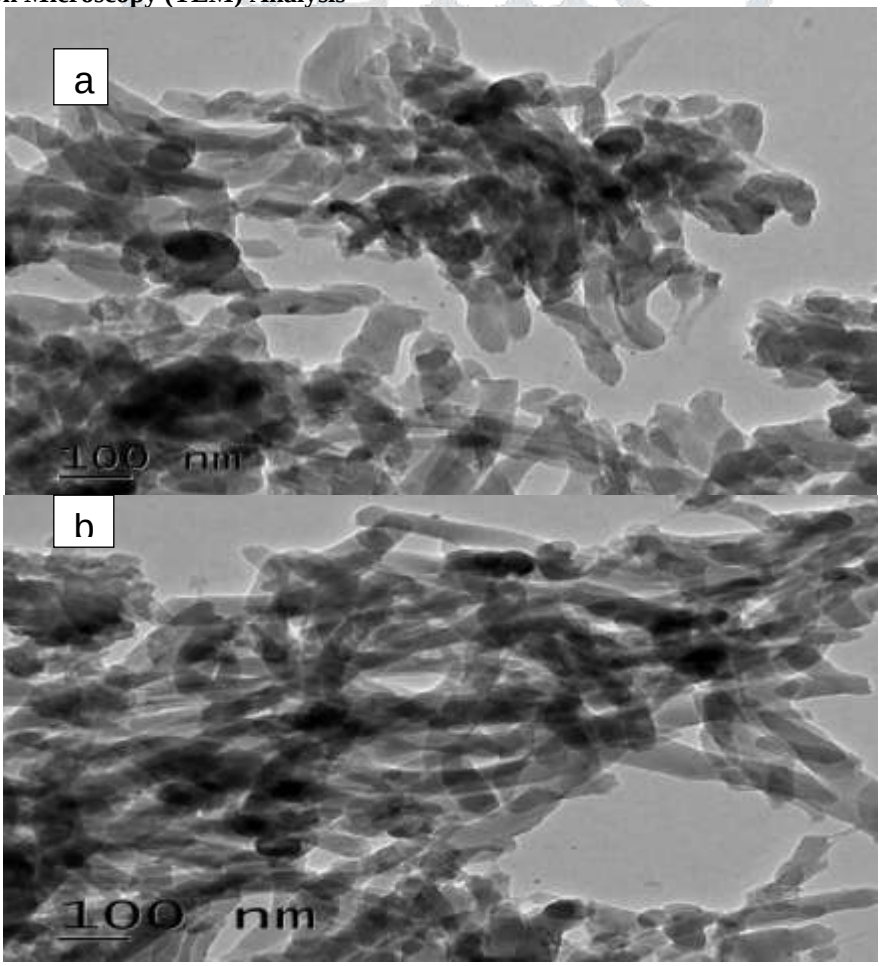

Fig 4. TEM micrographs of PANI: (a) Nano PANI-HCl (b) Nano PANI-TSA.

The transmission electron micrograph (TEM) images of nano PANI-HCl and nano PANI-TSA are shown in Figures 4a and 4b respectively. The TEM images clearly show a fibrous like morphology with a diameter of 2 nm in the form of hollow nanorods. The formation of these polyaniline nanorods/nano fibers occurring interfacially at the junction of the organic and aqueous phase during the polymerization process

may be due to the controlled and limited availability of the aniline monomer. The limited amounts of aniline monomer molecules in the organic phase interacts with the oxidizing agent that is present in the aqueous phase.

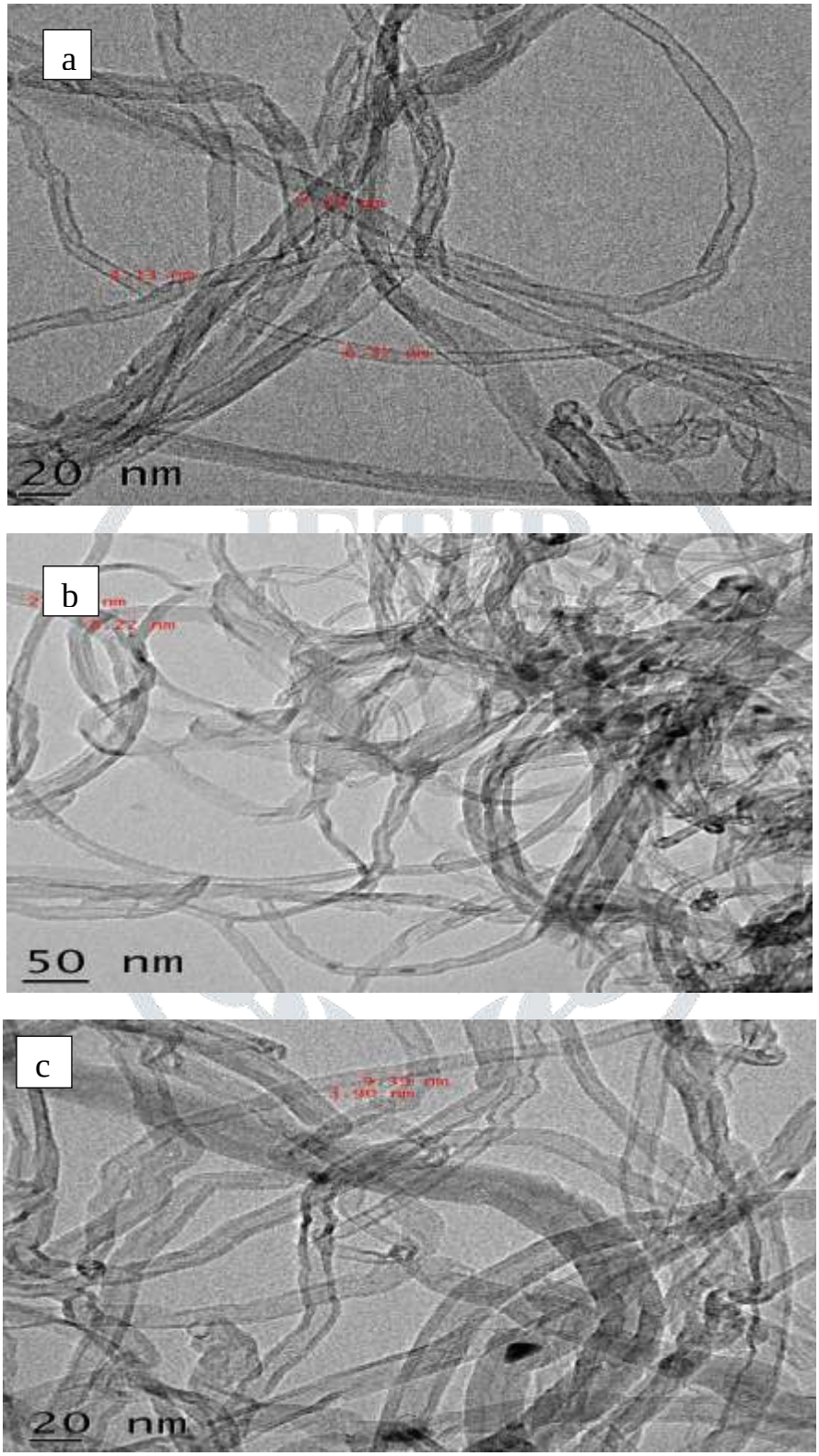

Fig 5. TEM micrographs of MWCNT: (a) Pristine CNT (b) ACNT (c) CCNT

The morphologies of pristine CNTs, ACNTs and CCNTs are shown in Figures 5a, 5b and 5c respectively. As shown in Figure 5a, the surface of the nanotube is smooth and the tubes are more or less uniform in size. The outer diameters of the MWCNTs ranges from 2 to 10 nm and their lengths are several micrometers. In the case of functionalized MWCNTs [Figures 5b and 5c], the surface is more rough which indicates the effective functionalization of nanotubes. Effective functionalization of MWCNTs can help to prepare a well dispersed solution of CNT in which the adsorption of aniline will be uniform and thus a thicker uniform coating of PANI can be impregnated on the dispersed CNTs [18].

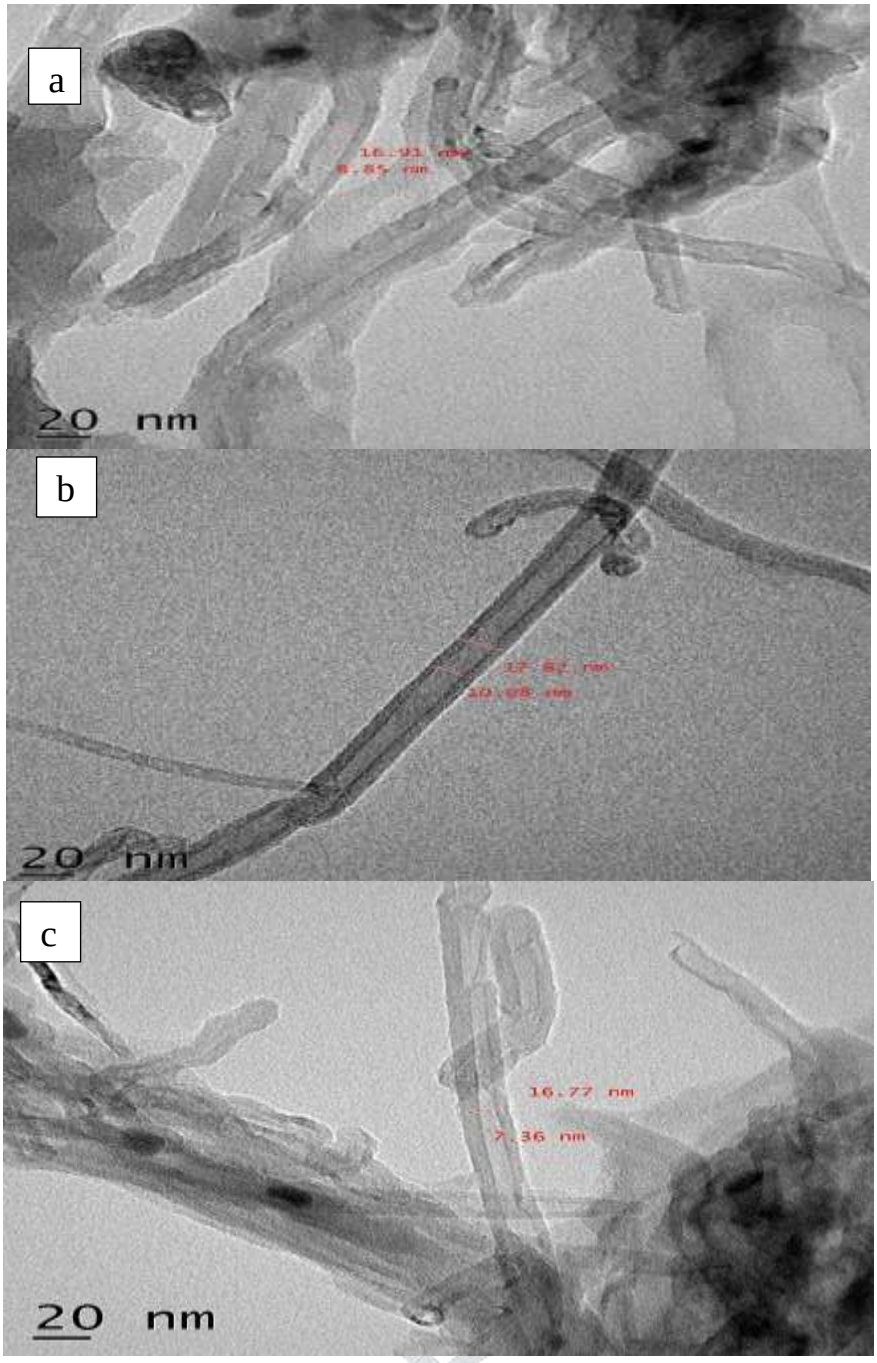

Fig 6. TEM micrograph of PANI-MWCNT: (a) PANI-Pristine CNT (b) PANI-ACNT (c) PANI-CCNT

The morphology of PANI-(pristine CNT, ACNT and CCNT) composites are shown in Figures 6a, 6b and 6c respectively. The Figures reveal that a uniform layer of PANI is formed on MWNTs' surfaces resulting in the enlargement of diameters to the range of 8 to 20 nanometers. Also the TEM images shows a marginal shortening of fibre lengths apparently due to a possible stripping of the sides of the MWCNTs fibres during sonication in aqueous solution of the dopant acid resulting in breakages and separation of the entangled fibres [19]. This disentanglement in the fibrous tubes tends to form a stable dispersion in water especially in the case of functionalized MWCNTs forming alignment which display a new interwoven fibrous structure which may give remarkable rise to conductive pathways and lead to high conductivity [20]. Since ACNT and CCNT are functionalized and can be well dispersed in the dopant solution compared to pristine CNT, a thick and uniform shell was formed on the surfaces of ACNT and CCNT as clearly observed in Figures 6b and 6c. Besides, the phenyl amino groups on the surface of ACNT is capable of initiating polymerization, the concentration of the monomeric species would be higher on the surface and hence, could lead to the formation of a thicker and more uniform coating of PANI on the surface of ACNT in the polymerization process [19-24].

3.3 Fourier Transform Infrared (FTIR) Spectroscopy

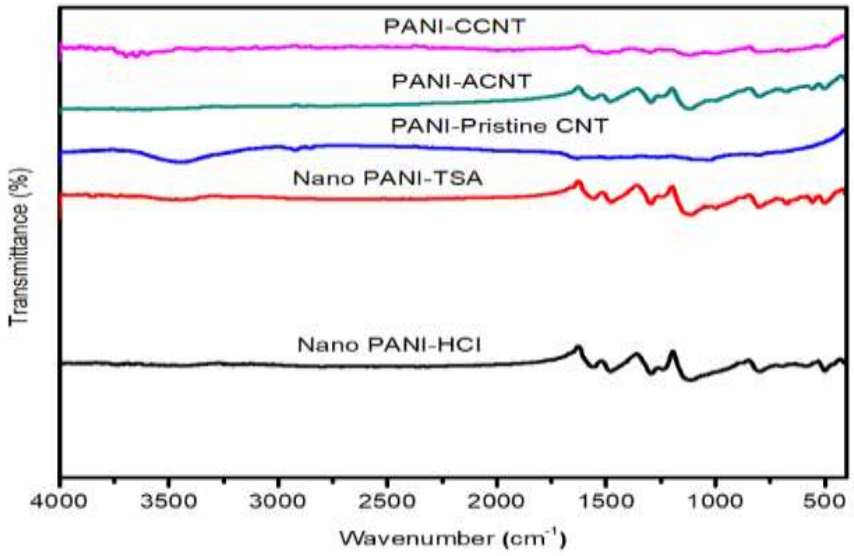

Fig. 7 FTIR Spectrum of Nano PANI-HCl, Nano PANI-TSA, PANI-pristine CNT, PANI-ACNT and PANI-CCNT

The FTIR spectra of nano PANI-HCl, nano PANI-TSA, PANI-pristine CNT, PANI-ACNT and PANI-CCNT are presented in Figure 7. The respective bands at 1560cm^{-1}, 1557cm^{-1} and 1480cm^{-1}, 1477cm^{-1} observed in the spectra of nano PANI-HCl and nano PANI-TSA respectively are attributed to the C=C stretching of quinoid and benzenoid rings indicating the oxidation state of emeraldine salt PANI [25-28]. The typical peaks at 1293 cm^{-1} and 1240 cm^{-1} for nano PANI-HCl and 1296 cm^{-1} and 1233 cm^{-1} for nano PANI-TSA are attributed to the bending vibration of C-N for aromatic amines/imines and C-N^{+} stretching vibrations in the polaronic structures (displacement of π electrons) owing to differing conformation or charge configuration suggesting the presence of protonated conducting PANI induced by acid doping of the polymer [6, 21, 29, 30]. The band at around 1111 cm^{-1} observed for both nano PANI-HCl and nano PANI-TSA spectra are assigned to C-H in-plane bending vibration is considered to be the extent of the degree of delocalization of electrons and thus it is the characterized peak of PANI [26]. The observed band at 769 cm^{-1} and 878 cm^{-1} in nano PANI-HCl and 697 cm^{-1} and 800 cm^{-1} in nano PANI-TSA respectively can be assigned to the aromatic ring out-of-plane deformation vibration bending of C-H bond in the benzene ring and para-distributed aromatic rings indicating polymer formation [21]. Out of plane bending deformation of C–H is observed at 506 cm^{-1} and 500 cm^{-1} in nano PANI-HCl and nano PANI-TSA respectively. The peak at 997 cm^{-1} in nano PANI-TSA can be assigned to SO_3^- group of the dopant TSA bound to the aromatic rings [27, 28]. The weak and broad signal observed at 3448 cm^{-1} in nano PANI-TSA also is assigned to N-H bond stretching indicating the presence of a secondary amine. This peak is broad and weak such that it is not visible in the nano PANI-HCl spectrum.

The figure also shows the interactions of PANI with MWCNTs in the nanocomposites. The peak at 1627 cm^{-1} is attributed to the C = C stretching, which indicates the graphitic structure of multi walled carbon nanotubes (MWCNTs). The bands at 1625 cm^{-1} and 1503 cm^{-1} in the spectra of ACNT are assigned to C-C stretching of carbon nanotube structure and C=O stretching of amide structure [16]. The peaks at 1555 cm^{-1} and 1365 cm^{-1} are attributed to N-H in-plane bending and C-N bond stretching vibrations respectively. The peak at 1630.78 cm^{-1} in the spectra of CCNT can be assigned to C=O stretching of the carboxylic acid functional group. The band at 1020.88 cm^{-1} may be assigned to C-O stretching vibrations of the carboxylic acid group [31] as well as adsorbed water. Also, the signals at 2855 cm^{-1} and 2924.47 cm^{-1} can be attributed to asymmetric CH_3 and symmetric CH_2 (C-H stretching respectively) [15, 32]. The peaks around 1555-1560 cm^{-1} and 3419 cm^{-1}-3426 cm^{-1} in the spectra of the three MWCNTs (pristine CNT, ACNT and CCNT) corresponds to the IR active phonon mode and OH stretching vibration of the MWCNTs [31]. The quinoid and benzenoid ring in the band of PANI at 1557 cm^{-1} and 1477 cm^{-1} is shifted to 1623 cm^{-1} and 1561 cm^{-1}, 1564 cm^{-1} and 1488 cm^{-1}, 1483 cm^{-1}, and 1503 cm^{-1} in the spectra of PANI-pristine CNT, ACNT and CCNT nanocomposites respectively. The shifting of the band confirms the interactions of the MWCNTs with the quinoid ring of PANI. The intensity of some of the signals in the nanocomposites were diminished compared to the pure PANI. The reason of decreased intensity is presumed to the adsorption of unreacted aniline monomer onto the surface of the MWCNTs limiting the growth of polymer chains around the nanotubes [26]. This constrained motion of the polymer chains and adsorption of monomeric aniline may limit the modes of vibration in PANI. Also, in acid solution, the NH_2 groups get protonated and becomes $+NH_3$ making the surface of the nanotubes positively charged. This in turn helps in achieving easy dispersion of CNTs in the nanocomposite due to mutual repulsion of positively charged PANI coated nanotubes [13].

3.4 X-Ray Diffractometry (XRD)

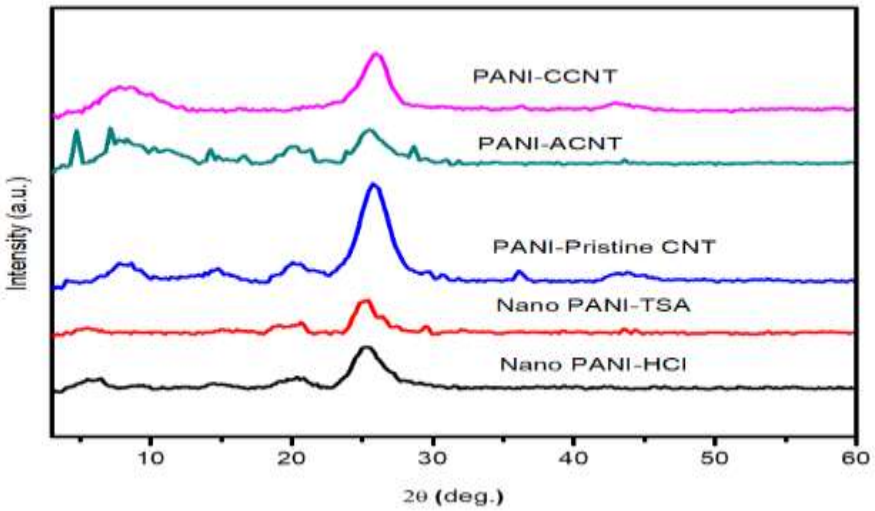

Fig. 8 XRD Pattern of Nano PANI-HCl, Nano PANI-TSA, PANI-pristine CNT, PANI-ACNT and PANI-CCNT

Figure 8 shows the XRD pattern of nano PANI-HCl, nano PANI-TSA, PANI-pristine CNT, PANI-ACNT and PANI-CCNT. The diffraction pattern of nano PANI-HCl are obtained at 2θ = 6°, 25° and 31°. The peaks give evidence for the partially crystalline nature of HCl doped PANI with conducting metallic islands separated by large amorphous regions. The diffraction pattern of the para-toluene sulphonic acid (TSA) doped nano PANI with sharp peaks at 2θ =20°, 25°, 28°, 43° and 44° also indicate the partial crystallinity of the sample. The sharp peak at 2 θ = 29° is a characteristic peak indicating the rigidity and well-ordered nature of some portion of PANI sub chains due to interchain packing between poly-cation and TSA anion [6, 9, 25, 33, 34]. The sharp peak at 2θ = 25° obtained for the two PANI samples is the characteristic peak of PANI indicating the extent of π conjugation in the polyaniline and sharpness of the peak reveals the degree of order of π conjugation.

PANI-MWCNTs (pristine CNT, ACNT and CCNT)) nanocomposites shows a strong and sharp diffraction peak identified for all samples at 2θ = 25° which is assigned (002) reflection. These peaks prominently appears at 26.2°, 25.87° and 25.93°. Pristine CNT and CCNT shows very broad peaks at 9.34° and 8.14° respectively with the peaks of CCNT showing a stronger and sharper peak. However, the three MWCNTs shows small island of peaks at 43° indicating (110) graphitic reflections from the nanotubes [26, 28, 35-37]. The slight peak shift observed at 25.87° and 25.93° in the functionalized MWCNTs viz., ACNT and CCNT suggests a strain on the surface of the nanotubes due to surface functionalization [38-40]. Also, the diffraction peaks of functionalized CNTs have become stronger and sharper compared to the pristine CNT. The X-ray diffractograms of PANI–MWCNTs composites show all the peaks corresponding to PANI as well as the MWCNTs, indicating that no additional crystalline order is introduced in these composites. The diffractograms show a highly pronounced structure of the primary doped PANI superimposed in the MWCNTs peaks, showing crystalline peaks at 25˚ with high intensity and sharpness especially the peaks of PANI- pristine CNT and carboxylic acid functionalized (CCNT)). The appearance of diffraction peak at 25˚ is common in both PANI and the MWNTs, indicating that MWCNTs are dispersed in the PANI matrix [41-44].

3.5 UV-Visible spectroscopy (UV-Vis)

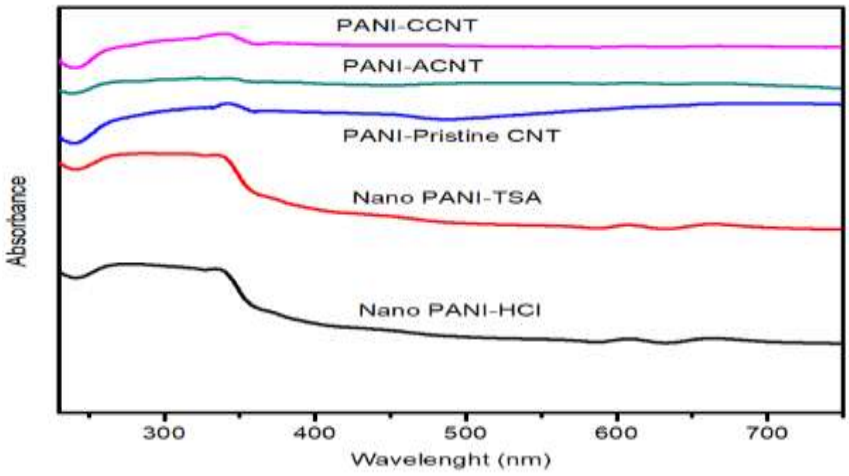

Fig. 9 UV-Visible Spectra of Nano PANI-HCl, Nano PANI-TSA, PANI-pristine CNT, PANI-ACNT and PANI-CCNT.

Electronic absorption of conducting polymers is useful in investigating the oxidation and doping state of the polymer. The UV-Visible spectra of nano PANI-HCl and nano PANI-TSA, PANI-pristine CNT, PANI-ACNT and PANI-CCNT are shown in Figure 9. Two absorption bands at 277–288 nm and 608–663 nm are obtained for both samples. The band at 277–288 nm in the nano PANI-HCl and nano PANI-TSA spectra are due to π-π* transitions in the benzenoid rings of polymer backbone while the band at 608–663 nm is due to exciton absorption of quinoid rings (n–π*) (inter-band charge transfer associated with excitation of benzoid (HOMO) to quinoid (LUMO) moieties) and a small shoulder-like band at 335 nm attributable to the formation of polaronic/bipolaronic transitions resulting in protonation of the polymer, indicating that the resulting PANIs are in the doped state [6, 21, 29, 30]. The continuous absorption peak at 780-790 nm shows free carrier tail, confirming the presence of conducting emeraldine salt phase of the polymer [45]. The slight difference in the absorption bands observed in the two PANI samples might be due to the molecular interaction of the dopants with imine nitrogen of PANI [35] resulting in the slight shift in absorption values. The nano PANI with comparatively larger particles as seen in SEM micrograph which may induce more specular reflection, hence lower absorption and blue shift. This could also influence the conductivity of the samples.

In the UV-Vis spectra of PANI–MWCNTs (pristine CNT, ACNT and CCNT) nanocomposites, the peak at around 260 nm in the PANI spectrums is shifted to higher wavelengths for the PANI-MWNCTs indicating a lower energy for the π–π* electronic transitions [42]. The spectrums of the composites exhibits both blue shift for PANI and red shifts for the MWCNTs with characteristic absorption bands at 341, 322 and 341 nm respectively. The shifting (blue and red) is attributed to the increased delocalization of charge carriers and charge transfer (CT) interaction between PANI and MWCNTs composites nanostructure which is believed to involve a strong interaction between aniline monomer and MWCNTs due to the presence of the π–π* electron as well as the hydrogen bond interaction between MWCNTs and the amino groups of aniline monomers enhancing charge transfer from quinoid unit of PANI to nanotubes. Such strong interaction resulting from the presence of MWCNTs in the composites ensures that the aniline monomer is adsorbed on the surface of MWCNTs, which serve as the core and self-assembly template during the formation of the tubular nanostructure [46]. Such shifts of the π–π* band in PANI-MWCNT composites compared to the PANIs is suggested to be due to the site-selective interaction between the quinoid ring of the PANI and CNTs. When PANI coats over the MWCNTs, the interfacial interaction between the two causes the π–π* transition to shift to a lower wavelength while at the same time, the absorption peak due to the polaron/bipolaron transition is red shifted in PANI-MWCNT composites compared to neat PANIs. Consequently, such a hypsochromic shift of the π–π* band is expected to result to a higher electrical conductivity for the PANI-MWCNT composites compared to the neat PANIs [38].

3.6 Thermogravimetric analysis (TGA) of Polyaniline

The thermogravimetric analysis (TGA) of PANI and PANI composites were conducted using a three-step weight-loss characteristic at constant degradation temperatures to ascertain their thermal stability and presented in Figure 10.

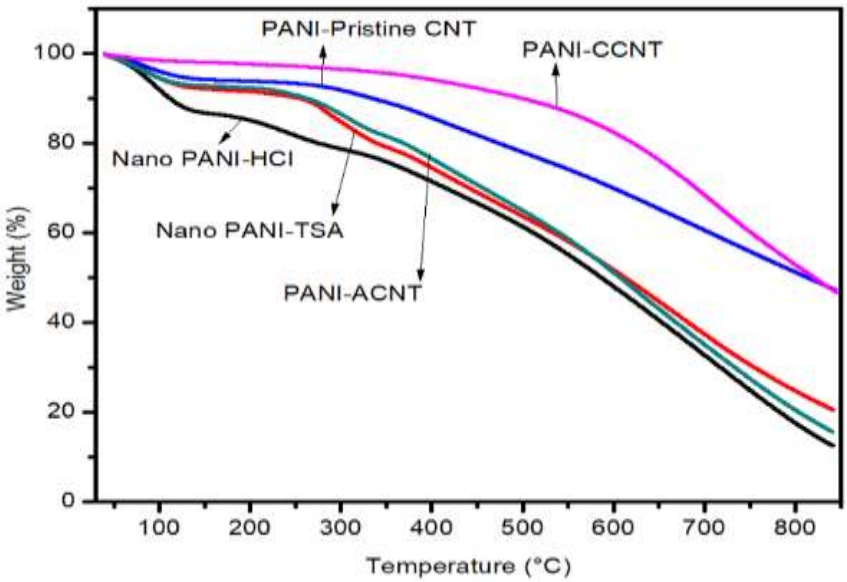

Fig. 10 TGA thermogram of Nano PANI-HCl, Nano PANI-TSA, PANI-pristine CNT, PANI-ACNT and PANI-CCNT

Figure 10 shows the TGA thermogram of nano PANI-HCl, nano PANI-TSA, PANI-pristine CNT, PANI-ACNT and PANI-CCNT. In the first step, approximately 10% and 6% weight loss respectively at the temperature up to 105°C can be seen in the thermogram of nano PANI-HCl and nano PANI-TSA respectively. This is attributable to loss of water molecules and unreacted organic monomers and the free acid trapped in the PANI structure [26, 34, 42]. The second weight loss of about 14% and 9% at temperature in the region of 220°C may be due to evaporation of dopant acids in PANI samples while the third step of weight loss was marked out at between 500°C and 800°C with 38%, 36% and 18%, 25% weight loss and residues respectively. This possibly represents the oxidative degradation of the PANIs which could be an indication of chemical structure decomposition resulting in chain scission [36]. The thermal behaviour of the two PANI samples is not much different from each other as observed in the thermograms.

The TGA thermogram of PANI-MWCNTs (pristine CNT, ACNT and CCNT) composites helps to determine the effect of MWCNTs on the thermal stability of PANI and verse-versa. In the first step, approximately 5%, 8%, and 1% weight loss respectively was observed at the

temperature up to 105°C as can be seen in the thermogram. This is as well attributable to loss of water molecules and unreacted organic monomers from the PANI-MWCNTs composite structure. The second weight loss of about 7%, 11% and 3% at temperature in the region of 220°C may be due to evaporation of dopant acids and low molecular weight oligomer in the PANI composites [26, 47]. The third step of weight loss usually referred to as oxidative degradation and decomposition temperature at between 500°C and 800°C has 21%, 35%, 10% and 51%, 21%, 53% weight loss and residues respectively for the three composites. The weight loss at all stage is much less for PANI-MWCNT nanocomposites compared to that of pure PANIs (nano PANI-HCl and nano PANI-TSA). These degradation patterns of the PANI-MWCNT nanocomposites indicates the superior thermal stability which was due to the ordered structure of MWCNTs [48, 49].

3.7 Electrical Conductivity Measurements

The electrical conductivity of pelletized nano PANI-HCl and nano PANI-TSA are found to be 0.478 and 0.824 S/cm^{-1} respectively. PANI doped with TSA possessed the highest conductivity. This is attributable to molecular composition of TSA which could have helped to stabilize the bond linking the dopant TSA and the polymer resulting from strong intermolecular interaction between aniline and counteranion molecules through the benzene ring of the dopant anion when TSA is incorporated [50, 51]. This will facilitate the formation of a resonating structure thereby activating electron flow in the form of polaron over the whole structure of the polymer chain. Also, the sulfur content of the TSA dopant anions may have contributed to the molecular interactions resulting in higher conductivity [52].

Table 1. DC conductivity of PANI-(pristine CNT, ACNT and CCNT) composites as a function of weight ratio of PANI.

Ratio of MWCNTs in 200mg of PANI	Conductivity (S/cm)		
	Pristine CNT	ACNT	CCNT
1:0.25	0.85	1.37	0.55
1:0.50	0.64	0.97	0.94
1:0.75	0.85	0.76	0.91
1:1	1.14	0.42	4.17
1:1.25	0.80	0.31	1.86
1:1.50	1.66	0.18	1.48

The conductivity of PANI-MWCNTs (pristine CNT, ACNT and CCNT) respectively as a function of weight ratio of MWCNTs is presented in Table 1. The conductivity of the composites is greatly improved by the introduction of MWCNTs in the PANI compared to values obtained for neat PANI. The composites exhibited an order of magnitude increase in electrical conductivity with increase of the CNT content up to at a ratio 1:1 especially of CCNT and PANI where a threshold of over 4.2 S/cm was observed. The measured increase in conductivity of the composites may be due to a doping capability of carbon nanotubes where the nanotubes tends to compete with sulfonic ion. MWNTs may serve as conducting bridges between scattered islands of PANI, thereby boosting charge delocalization [18]. The improved crystallinity of PANI with the addition of MWNT is another possible reason for the increase in conductivity across the PANI-MWCNT nanocomposites. However, it is observed that the composites containing functionalized MWCNTs (carboxylic acid and amine) were more stable and regular in the conductivity values compared to the pristine CNT.

4.0 CONCLUSION

PANI in nano dimensions could be prepared through chemical oxidative polymerization of aniline using HCl or TSA as dopants. Nanocomposites of PANI and MWCNTs (pristine CNT, ACNT and CCNT) could be prepared by in situ polymerization using TSA dopant. The SEM and TEM studies show that the nano PANIs are in nano dimension while PANI-MWCNTs nanocomposites show adherence of the MWCNTs to PANI matrix by the formation of core-shell acting as a charge-transfer linkage. The TGA data indicates better enhancement of the thermal stability of nano PANI doped with TSA compared to the nano PANI doped with HCl. The thermal stability of the PANI-MWCNTs nanocomposites indicates that the thermal stability of the PANI can be enhanced by the incorporation of MWCNTs. The electrical conductivity of PANI can be enhanced by the incorporation of MWCNTs. Among the nanocomposites studied, the highest electrical conductivity was observed in PANI-MWCNTs (CCNT) at ratio 1:1, where the intermolecular interactions between the constituents are stronger than in the other nanocomposites studied.

REFERENCE

[1] Shirakawa H, Lewis EJ, MacDiarmid AG, et al. 1977. Synthesis of electrically conducting organic polymers: halogen derivatives of polyacetylene (CH)x. J Chem Soc, Chem Comm, 16 578-580.

[2] Sadia Ameen, Shaheer M Akhtar, Minwu Song and Hyung Shik Shin 2013. Solar cells - research and application perspectives. In: Arturo Morales-Acevedo (eds) Metal oxide nanomaterials, conducting polymers and their nanocomposites for solar energy. InTech, pp.203-259.

[3] Srinivasan Palaniappan and Amalraj John 2008 Polyaniline materials by emulsion polymerization pathway. Prog Polym Sci, 33 732-758

[4] Bakhishi AK and Geetika Bhalla 2004. Electrically conducting polymers: materials of the twenty-first century. J Sci and Ind Res, 63 715-728

[5] Stejskal J and Gilbert RG 2002 Polyaniline: preparation of a conducting polymer. Pure Appl Chem, 74 (5) 857-867

[6] Sewench N Rafeeq and Wasan Z Khalaf 2015. Preparation, characterization and electrical conductivity of doped polyaniline with (HCL and P-TSA). The 5th International Scientific Conference for Nanotechnology and Advanced Materials and their Applications ICNAMA 2015, pp.3-4.

[7] Yongfang Li 2015. Organic optoelectronic materials, Yongfang Li (ed.), Springer International Publishing Switzerland, Lecture Notes in Chemistry 91, DOI 10.1007/978-3-319-16862-3.

[8] Bingqing Yuan, Liming Yu, Leimei Sheng, et al. 2012. Comparison of electromagnetic interference shielding properties between single-wall carbon nanotube and graphene sheet/polyaniline composites. J Phys D: Appl Phys, 45 (23).

[9] Estabraq T Abdullah, Salma M Hassan and Reem S Ahmed 2016. Electrical properties of polyaniline/functionalized multi walled carbon nanotubes nanocomposite. Int J Curr Engg Tech 6 (2).

[10] Iijima S 1991. Helical microtubules of graphitic carbon. Nature, 354 (6348) 56-58.

[11] Gogotsi Y, Naguib N, and Libera JA 2002. In situ chemical experiments in carbon nanotubes. Chem Phys Letts 365 354-360.

[12] Ya-Ping Sun, Weijie Huang, Yi Lin, et al. 2001. Soluble dendron-functionalized carbon nanotubes: preparation, characterization and properties. Chem Mater 13 (9).

[13] Liqiang Cui, Junsheng Yu, Yinghai Lv, et al. 2013. Doped polyaniline/multiwalled carbon nanotube composites: preparation and characterization. Soc Plasts Engrs, Polym Comps, 34 (7) 1119-1125.

[14] Van Thu Le, Cao Long Ngo, Quoc Trung Le, et al. 2013. Surface modification and functionalization of carbon nanotube with some organic compounds. Adv Nat Sci: Nanosci. Nanotech., 4 (3).

[15] Wellington M Silva, Hélio Ribeiro, Luciana M Seara, et al. 2012. Surface properties of oxidized and aminated multi-walled carbon nanotubes. J Braz Chem Soc., 23 (6) 1078-1086.

[16] Eren O, Ucar N, Onen O, et al. 2014. Effect of amine-functionalized carbon nanotubes on the properties of CNT-PAN composite nanofibers. J Chem and Mol Eng., 8 (8).

[17] Singubiru M Khatake, Mathe VL and Girish M Joshi 2015. Grafting of amine-functionalized multiwall carbon nanotubes with free acid anhydride in carboxylic acid modified epoxy. Polym-Plasts Tech and Eng., 54 (8) 851-860.

[18] Arup Choudhury and Pradip Kar 2011. Doping effect of carboxylic acid group functionalized multi-walled carbon nanotube on polyaniline. Composites: Part B, 42 1641–1647.

[19] Shahnawaza S, Sohrabi B and Najafib M 2014. The investigation of functionalization role in multi-walled carbon nanotubes dispersion by surfactants. In proceedings of the 18th Int Electron Conf Synth Org Chem 2014; 1-30

[20] Lu KL, Lago RM, Chen YK, et al. 1996. Mechanical damage of carbon nanotubes by ultrasound. Carbon, 34 (6) 814-816.

[21] Bachhav SG and Patil DR 2015. Synthesis and characterization of polyaniline-multiwalled carbon nanotube nanocomposites and its electrical percolation behavior. Amer J Mats Sci., 5 (4) 90-95.

[22] Ben-Lin He, Bin Dong, Wei Wang and Hu-Lin Li 2009. Performance of polyaniline/multi-walled carbon nanotubes composites as cathode for rechargeable lithium batteries. Mats Chem and Phys., 114 371-375.

[23] Thomassin JM, Jérôme C, Pardoen T, et al. 2013. Polymer/carbon based composites as electromagnetic interference (EMI) shielding materials. Mats Sci and Engg R., doi.org/10.1016/j.mser.2013.06.001

[24] Yi-bo Zhao, Wei Wu, Jian-feng Chen, et al. 2012. Preparation of polyaniline/multiwalled carbon nanotubes nanocomposites by high gravity chemical oxidative polymerization. Amer Chem Soc Publ: Ind Eng Chem Res., 51 3811-3818.

[25] Haisel Mathew, Vrinda S Punnackal, Sunny Kuriakose, et al. 2013. Synthesis and electrical characterization of polyaniline-multiwalled carbon nanotube composites with different dopants. Int J Sci and Res Publ., 3 (8).

[26] Anil Kumar, Vinod Kumar, Manoj Kumar and Kamlendra Awasthi 2017. Synthesis and characterization of hybrid PANI/MWCNT nanocomposites for EMI applications. Polym Comps., **1** DOI 10.1002/pc.24418

[27] Estabraq T Abdullah, Reem S Ahmed, Salma M Hassan and Asama N Naje 2015. Synthesis and characterization of PANI and polyaniline/multi walled carbon nanotube composite. Int J Applic Innov Engg & Mgt., 4 (9).

[28] Ratheesh R and Viswanathan K 2014. Chemical polymerization of aniline using para-toluene sulphonic acid. IOSR J Appli Phys., 6 (1) Ver. II, 1-9.

[29] Goutam Chakraborty, Kajal Gupta, Dipak Rana and Ajit Kumar Meikap 2012. Effect of multiwalled carbon nanotubes on electrical conductivity and magnetoconductivity of polyaniline. Adv Nat Sci: Nanosci. Nanotechnol., 3 (3).

[30] Veluru Jagadeesh Babu, Sesha Vempati and Seeram Ramakrishna 2013. Conducting polyaniline-electrical charge transportation. Mats Sci and Appls., 4 1-10.

[31] Jeevananda T, Siddaramaiah Hatna, Nam Hoon Kim, et al. 2008. Synthesis and characterization of polyaniline-multiwalled carbon nanotube nanocomposites in the presence of sodium dodecyl sulfate. Polym Adv Technol., 19 1754-1762.

[32] Zhiyuan Zhao, Zhanhong Yang, Youwang Hu, et al. 2013. Multiple functionalization of multi-walled carbon nanotubes with carboxyl and amino groups. Appl Surf Sci., 276 (1) 476-481.

[33] Tzong-Ming Wu and Yen-Wen Lin 2006. Doped polyaniline/multi-walled carbon nanotube composites: preparation, characterization and properties. Polymer, 47 3576-3582.

[34] Pandi Gajendran and Ramiah Saraswathi 2008. Polyaniline-carbon nanotube composites. Pure Appl Chem., 80 (11) 2377-2395.

[35] Mohamad Khalid, Milton A Tumelero, Iuri. S Brandt, et al. 2013. Electrical conductivity studies of polyaniline nanotubes doped with different sulfonic acids. Indian J Mats Sci., Vol 2013, doi.org/10.1155/2013/718304.

[36] Zhang JQ, Shi CM, Ji TZ, et al. 2014. Preparation and microwave absorbing characteristics of multi-walled carbon nanotube/chiral-polyaniline composites. Open J Polym Chem., 4 62-72

[37] Motomichi Inoue, Castillo-Ortega M Monica and Michiko B Inoue 1997. Polyaniline toluenesulfonates: X-Ray diffraction and electrical conductivity. J.M.S.-Pure Appl Chem., 34 (8) 1493-1497.

[38] Jelmy E Johny, Ramakrishnan S, Murali Rangarajan and Nikhil K Kothurkar 2013. Effect of different carbon fillers and dopant acids on electrical properties of polyaniline nanocomposites. Bull. Mater Sci., 36 (1) 37-44.

[39] Mohd Pauzi Abdullaha, and Siti Aminah Zulkepli 2015. The functionalization and characterization of multi-walled carbon nanotubes (MWCNTs). AIP Conference Proceedings 1678 doi.org/10.1063/1.4931312.

[40] Duha S Ahmed, Adawiya J Haider and Mohammad MR 2013. Comparison of functionalization of multi-walled carbon nanotubes treated by oil olive and nitric acid and their characterization. Terra Green 13 International Conference 2013 - Advanmts Renew Energ Clean Env, Energy Procedia, 36 1111 – 1118.

[41] Katherine Calamba, Cherry Ringor, Chelo Pascua and Kunichi Miyazawa 2014. Pleated surface morphology of C60 fullerene nanowhiskers incorporated by polyaniline in N-methyl-2-pyrrolidone. Fullerenes, Nanotubes and Carbon Nanostructures, 23 (8) 709-714.

[42] Faris Yılmaz and Zuhal Kuqukyavuz 2009. Conducting polymer composites of multiwalled carbon nanotube filled doped polyaniline. J Appl Polym Sci., 111 680-684.

[43] Pradyumna Mogre, Sharanabasava V Ganachari, Jayachandra S Yaradoddi, et al. 2018. Synthesis and characterization studies of polyaniline nano fibres. Adv Mats Proceedings, 3 (3), 178-180.

[44] Adawiya J Haider, Mohammed MR and Duha S Ahmed 2014. Preparation and characterization of multi walled carbon naotubes/Ag nanoparticles hybrid materials. Int J Sci & Engg Res 5 (3).

[45] Milind V Kulkarni and Bharat B Kale 2012. Development of optical pH sensor using conducting polyaniline-wrapped multiwalled carbon nanotubes (PANI-MWCNTs) nanocomposite. IMCS 2012 - The 14th International Meeting on Chemical Sensors, DOI 10.5162/IMCS2012/P1.3.2.

[46] Tomova A, Gentile G, Grozdanov A, et al. 2016. Functionalization and characterization of MWCNT produced by different methods. ACTA Phys Pol A, 129 (3) DOI: 10.12693/APhysPolA.129.405.

[47] Elsayed AH, MohyEldin MS, Elsyed AM, et al. 2011. Synthesis and properties of polyaniline/ferrites nanocomposites. Int J Electrochem Sci 6 206-221.

[48] Ghatak S, Chakraborty G, Meikap AK, et al. 2011. Synthesis and characterization of polyaniline/carbon nanotube composites. Journal of Appl Polym Sci., 119 1016-1025.

[49] David T, Jyotsna Kiran Mathad, Padmavathi T and Vanaja A 2014. Synthesis of polyaniline (PANI) and PANI/c-SWCNT composites for EMI coatings. Polymer, 55 (22).

[50] Narayan Chandra Das, Shinichi Yamazaki, Masamichi Hikosaka, et al. 2005. Electrical conductivity and electromagnetic interference shielding effectiveness of polyaniline ethylene vinyl acetate composites. Polym Int 54 256-259.

[51] Chutia P and Kumar A 2014. Electrical, optical and dielectric properties of HCl doped polyaniline nanorods. Physica B, 436 200-207.

[52] Xiao Wang, Sudip Ray, Marija Gizdavic-Nikolaidis and Allan J Easteal 2012. The effects of dopant acids on structure and properties of poly(o-methoxyaniline). J Polym Sci Part A: Polym Chem., 50 353-361.